Veterinary Radiology & Ultrasound

WILEY

ORIGINAL RESEARCH

Ultrasonographic Assessment of the Lungs in Asiatic Elephants (*Elephas maximus*)

Nirmali Sarma | Tenzing L. Lachenpa | Yaduraj Khadpekar | Vaisakh Viswam | Jahan Ahmed | Niraj Dahe | Akshay Ghatare | Govind Shankar | Nikorn Thongtip | Shubham Patil

Radhe Krishna Temple Elephant Welfare Trust, Vantara, Jamnagar, Gujarat, India

Correspondence: Nirmali Sarma (nirmali.sarma@KW-TRUST.org; dr.ninasarma@outlook.com)

Received: 13 August 2025 | **Revised:** 2 December 2025 | **Accepted:** 21 May 2026

Keywords: Asian elephant | diagnostic imaging | lung mapping | lung ultrasound score

ABSTRACT

Asian elephants possess a unique pulmonary anatomy that presents challenges for diagnosing respiratory diseases, particularly when reared under human care where environmental stressors, poor hygiene and limited physical activity predispose them to respiratory pathologies. Conventional diagnostic tools such as radiography, computed tomography (CT), and magnetic resonance imaging (MRI) are impractical for elephants due to their large body size. Diagnosis of lung pathologies is often delayed until postmortem. This study evaluated the diagnostic utility of lung ultrasound (LUS) as a noninvasive, real-time imaging modality in assessing lung health in Asian elephants. A total of 68 noncardiac transthoracic ultrasound scans were performed on 28 elephants to develop a systematic approach for pulmonary imaging. LUS demonstrated high sensitivity in detecting lung lesions, including interstitial syndrome, pulmonary edema, consolidation, pneumothorax, and pleural effusion, even in apparently healthy, asymptomatic individuals. Specific thoracic zones serving as acoustic windows were successfully mapped to improve consistency in lesion localization. Additionally, a semi-quantitative LUS score was developed for the objective assessment of lung aeration across 24 thoracic regions. Despite species-specific challenges such as narrow intercostal spaces and large lung volume, key sonographic features, including A-lines, B-lines, lung sliding, and bronchograms, were visualized. This study establishes LUS as a practical, field-adaptable tool for antemortem detection and monitoring of respiratory disease in elephants. Its ability to detect subclinical pathology offers significant benefits for early intervention, improved clinical outcomes, and support for conservation efforts. LUS has the potential to transform pulmonary diagnostics in elephant healthcare, bridging a critical gap in veterinary medicine for this endangered species.

1 | Introduction

Asian elephants (*Elephas maximus*), among the largest terrestrial mammals, exhibit a distinctive pulmonary anatomy that complicates the diagnosis of respiratory pathologies, especially within managed populations. The lung of the elephant, when separated from the thoracic cavity, is covered by a thick, dense visceral pleura. The parietal pleura is also thick and dense. However, a proper pleural cavity between the parietal and visceral layers is absent [1]. The lung architecture in African elephants exhibits a very thick parietal pleura even in the fetal stage, as part of an early-developed endothoracic fascia spanning hundreds of micrometers by mid-gestation. This suggests structural adaptations preparing the animal for snorkeling and suction behavior after birth. Although the fetal lungs initially have a separate pleural cavity, this cavity fuses just before birth; in neonates and adults, there is effectively no pleural space, and lung tissue is directly adhered to the chest wall and diaphragm via connective tissue [2].

Spanning from the second to 16th rib, the right lung in Asian elephants is larger than the left, which ranges from the third to 16th rib, observed in a stillborn Asian elephant fetus [3] with anatomical details of the parietal and visceral pleura similar to African elephant fetus [2]. The left lung has two lobes: the apical and the diaphragmatic. The right main bronchus of the elephant has four divisions; thus, the right lung presents four lobes—apical, cardiac, mediastinal, and diaphragmatic. The cardiac notch on the left lung appears much smaller than that of the right lung in elephants. The left notch has an acute angle, whereas the right possesses an obtuse angle. Unlike the more vertically oriented diaphragms seen in other animals, the elephant's diaphragm lies at an oblique angle of approximately 45° relative to the spinal axis and the direction of gravitational force [4]. The respiratory system of elephants is unique as it lacks a typical pleural cavity [5]. The mobility, extreme compliance, ease of shearing, and slipperiness of the pleural space connective tissue (PSCT) in elephants imply that PSCT has no significant influence on lung sliding during breathing. Thus, the lung is free to slide relative to the chest wall, diaphragm, and mediastinum and move in and out of the costophrenic sulcus [4].

Elephants under human care often face environments that are unable to meet their complex physical, psychological, and social needs. Certain rearing conditions can often lack sufficient space, environmental requirements, and social structures, leading to stress-related behaviors such as stereotypies, obesity, foot, and dental problems [6]. These stressors can not only impair physical and psychological health but also predispose elephants to a range of clinical conditions, including respiratory disease. Poor ventilation, confined indoor spaces, and limited exercise can create conditions that compromise respiratory health, making elephants more susceptible to infections and chronic lung problems [7], as observed in some populations under human management [8]. When combined with chronic stress and limited exercise, these factors compromise respiratory immunity and lung function, raising concerns about lung health in elephants. A compromise in the quality of husbandry, healthcare, and management can contribute to a compromise in the health of elephants under human care.

Conventional diagnostic methods such as radiography, computed tomography (CT), and magnetic resonance imaging (MRI) are rendered largely impractical in elephant veterinary radiology, especially for individuals larger than calf-size, due to the sheer size of these animals and the logistical constraints of performing such procedures [9]. Many lung pathologies in elephants remain undiagnosed until postmortem examinations, as they often do not manifest in routine blood work, further complicating early detection and intervention. Auscultation of the elephant thorax presents notable challenges, largely due to the species' unique anatomy. The exceptionally thick thoracic wall, combined with extensive caudal lung fields and massive ribs, significantly dampens sound transmission and makes normal breath sounds difficult to detect with a standard stethoscope. As a result, even high-quality stethoscopes often provide limited clinical value [10]. The advent of veterinary clinical ultrasound has provided a new tool for assessing pulmonary health [11]; however, its potential in diagnosing lung pathologies in elephants remains largely untapped.

Modern veterinary medicine has witnessed the application of bronchoscopy for upper respiratory tract evaluation in elephants; however, it has presented several procedural challenges, primarily stemming from anatomical constraints and equipment limitations. Suitable endoscopic instruments of adequate length and diameter are often unavailable, making it difficult to navigate the extensive airway of these large mammals [12]. Accessing the trachea and bronchi via the nasal route is largely impractical due to the considerable length of the trunk, which greatly exceeds the reach of standard equipment. Consequently, oral access becomes necessary, yet this too is complicated by the elephant's distinctive craniofacial anatomy, including their powerful jaws, a short mandible, and substantial musculature at the base of the trunk. This restricts safe and controlled placement of endoscopes without specialized devices. These combined factors underscore the inherent complexity of performing respiratory endoscopy in elephants [13]. Moreover, endoscopy does not provide information on pleural integrity or accumulation of infiltrates in alveolar interstitial spaces.

Lung ultrasound (LUS) has recently emerged as a valuable diagnostic tool in veterinary radiology, offering a noninvasive, rapid, and bedside method for assessing pulmonary pathology in small and large domestic animals. Traditionally underutilized due to the belief that air-filled lungs were poorly suited to ultrasonography, LUS has gained attention for its sensitivity in detecting conditions such as pleural effusion, pulmonary edema, and interstitial-alveolar syndromes [14]. Its utility in veterinary medicine is still relatively new, with structured protocols and scoring systems such as the LUS score, which was only recently validated for dogs and cats [15]. This facilitates a shift in clinical practice, as the potential of ultrasound as an efficient diagnostic modality is now recognized not only in abdominal and cardiac imaging but also for dynamic, real-time pulmonary assessment, showing its reliability in emergency and critical care [16].

There are studies that suggest that LUS is an effective tool for detecting early or subclinical lung disease, often before symptoms emerge. It offers high sensitivity and specificity, making it a valuable, noninvasive, bedside screening method for early lung pathology in both human [17] and animal models [18].

This study explores the application of diagnostic ultrasonography in evaluating the lungs of elephants through 68 noncardiac transthoracic ultrasound scans conducted in 28 elephants to develop a systematic scanning technique for such a large organ, potentially filling a critical gap in elephant healthcare. Implementing ultrasound in elephant diagnostics could significantly improve the standard of care by enabling timely and precise diagnoses that were previously unattainable.

This study was undertaken with the following objectives:

1. To explore the feasibility and diagnostic utility of dynamic real-time ultrasound imaging for evaluating elephant lungs.

2. To assess the sensitivity and specificity of LUS in detecting pulmonary pathologies in elephants.
3. To develop anatomical reference zones for accurate mapping of lung lesions.
4. To create a practical and semi-quantitative scoring system for rapid assessment of elephant lung health: the LUS.

2 | Materials and Methods

The study was conducted at the Radhe Krishna Temple Elephant Welfare Trust, Jamnagar, Gujarat, India, a care and rehabilitation center for elephants under human care that were rescued from different states across the country. These elephants had spent the majority of their lifetime in managed care, a factor that can predispose them to a range of pathologies, including respiratory system disorders [7], the occurrence of which may vary regionally, depending on environmental and management conditions in some human-managed populations [19]. The study was carried out over 22 months, and a total of 28 adult Asian elephants (*E. maximus*) with ages ranging from 25 to 68 years (approximately) of both sexes were subjected to a detailed pulmonary health assessment using noncardiac transthoracic ultrasound. Prior to performing the procedure, patient history, clinical symptoms, and body condition scores (BCSs) [20] were noted. As the elephants were rescued, exact ages could not be obtained. A total of 13 out of 28 elephants were reported to exhibit clinical signs such as exercise intolerance, lethargy, frequent gaping of the mouth, and slow gait, in various degrees. The procedures conducted during the study were in compliance with the guidelines of humane treatment of animals and were approved by the Ethical Review Committee of Radhe Krishna Temple Elephant Welfare Trust.

2.1 | Patient Preparation

The elephants in the study were desensitized for the procedure using positive conditioning methods prior to the actual evaluation. This desensitization period varied for individual elephants, ranging from 1 to 4 weeks. The elephants were examined in "free contact" settings without sedation under minimal physical restraint. During the evaluation, two mahouts (elephant keepers) were positioned with one next to the head and the other at the rear of the elephant. One attendant offered fruits and vegetables as treats at regular intervals to keep the elephant calm and engaged.

The skin in the region of interest was dusted, brushed, and thoroughly washed with clean water delivered via a hose. The wrinkles on the skin were also cleaned with care to remove dust particles and prevent air trapping [21]. After thorough cleaning, acoustic gel was applied over the thoracic region to enable adequate contact between the transducer surface and skin, as well as to avoid trapping of air between hair strands (if any) and skin wrinkles. Some elephants with very coarse and dry skin were subjected to the application of coconut oil twice a day in the region of interest, 3–5 days prior to the scheduled date of evaluation. All the elephants in this study were examined in a standing position.

2.2 | Region of Interest

The elephant lungs are large organs and need to be evaluated over a broad area extending 58–63 cm from the caudal border of the scapula at the proximal region of the lung, gradually tapering downwards, extending only 33–41 cm from the caudal border of the humerus at the distal region of the lung, with size variations observed depending on the size of the animal. This triangular lung area can be traced using ultrasound, allowing a noninvasive estimation of lateral lung span. In Asian elephants, the right lung spans ribs 2–16, whereas the left ranges from ribs 3–16 [3]. Due to this large span of the lateral lung border and the size of the elephant, the thorax was divided into four zones with three imaginary lines drawn equidistant to each other, perpendicular to the median plane and parallel to the dorsal plane of the elephant's body (Figures 1 and 2a).

Each zone was then divided into three regions, namely, cranial, middle, and caudal, with two imaginary lines drawn perpendicularly to the dorsal plane and parallel to the median plane of the body (Figure 2a,b). This was done to map the different regions of the lung with more precision and locate lesions accurately in subsequent ultrasound scans. However, the cranial region of the thorax was not accessible from the lateral aspect due to the presence of the pectoral limbs. The scapula and humerus superimpose the cranial border of the lungs bilaterally, rendering it impossible to view through ultrasonography. The points of the triangular surface lung area on the lateral thoracic walls for ultrasonographic evaluation were from the caudal angle of the scapula (A) to the dorsal end of the 15th to 16th intercostal space (B) and the caudal border of the humerus at its distal third, in the arm region (C), as shown in Figure 2a,b.

2.3 | Ultrasonography

Noncardiac transthoracic ultrasonography was performed bilaterally to evaluate the lungs of the elephants. A portable ultrasound machine (Aeroscan CD10-Pro, Konica Minolta Pvt. Ltd.) equipped with a curvilinear transducer of 2–5 MHz frequency was used. No additional accessories were used for this procedure. When performed in field settings, the examinations were conducted in the evening to improve screen visibility. The focal point was at 20 cm, the total gain was 53, and the dynamic range was set to 56 for all scans.

The transducer was positioned on the skin over the lateral thoracic wall using the intercostal spaces as acoustic windows [22], as the ribs cast acoustic shadows. The transducer axis is held perpendicular to the skin surface [23] along the dorsal plane with the ultrasound beam directed towards the median plane (Figure 1) and probe marker positioned cranially (Figure 3). As both the thoracic wall and the transducer footprint are convex in shape, mild-to-moderate pressure was applied while scanning to obtain adequate contact.

Images were observed in brightness (B) and motion (M) mode. B-mode ultrasonography enabled visualization of internal structures in two-dimensional images, allowing the characteristic appearances of tissue and artifacts to be appreciated. M-mode displayed the pattern of movement of different structures in a

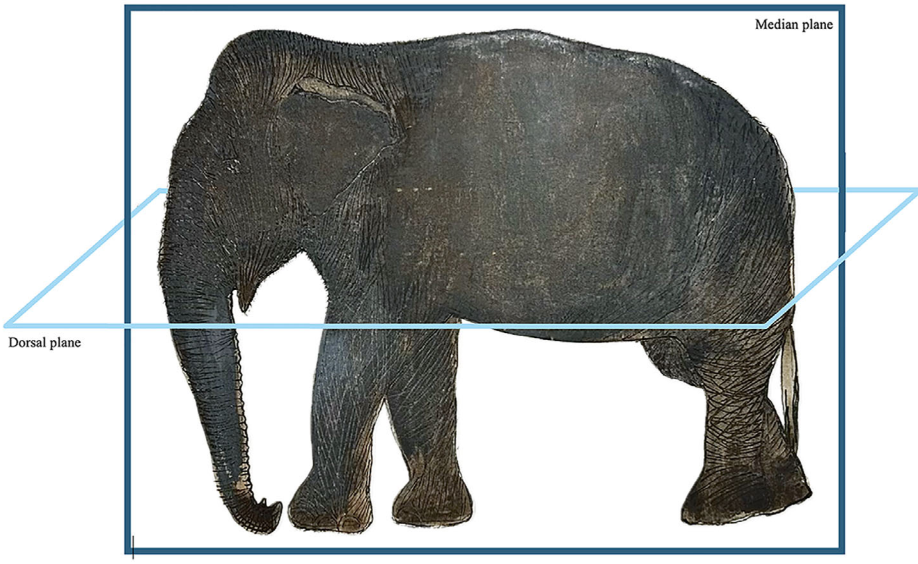

FIGURE 1 | Schematic diagram of an elephant's body with median and dorsal planes.

unidimensional format via real-time mapping of the amplitude and range of motion of target tissue encountering the beam of sound [24]. Each lung zone was examined in order starting at the proximal end and progressing to the distal end (Zones 1–4) and each zone was scanned from cranial to caudal direction (Figure 2a,b) with "fanning" [25] of beam upwards to downwards, directing the ultrasound towards dorsomedial and ventromedial directions in a sweeping pattern, for thorough screening of the tissues. The scanning procedure lasted up to 1 h in initial examinations, and 15 min to 1 h in follow-ups; the latter was planned based on the findings from the first LUS to monitor progression of disease and efficacy of treatment. The images were analyzed during the evaluation and often reviewed after the procedure, especially when the study was performed in field settings under bright daylight, to ensure that lesions, if any, did not go undetected due to screen glare.

3 | Results and Discussion

In the present study, all elephants participated in a period of positive-conditioning-based desensitization prior to ultrasonographic evaluation, as outlined in the Methodology. This method proved highly effective, as the elephants cooperated without interruptions or signs of behavioral discomfort throughout the procedures. The scans were performed in free-contact settings without sedation, relying only on minimal physical restraint and the reassuring presence of mahouts. Intermittent food rewards further helped keep the elephants relaxed and engaged, allowing the procedures to be completed smoothly and safely for both animals and handlers. However, acknowledging that other veterinary practitioners may face challenges working in facilities that manage elephants under "protected contact," elephants may be desensitized using positive conditioning techniques and guided to stand next to a treatment window, providing adequate access to the region of interest (Figure 2a,b). If the patient is prone to exhibiting aggression and does not allow us to be approached, it may be chemically immobilized and examined with standing sedation.

Of the 28 elephants, 5 had a BCS of <3. The remaining 23 elephants scored ≥3. The elephants with BCS of <3 also exhibited clinical signs as described before. Such clinical signs were also observed in eight elephants with a BCS of ≥3. However, using noncardiac transthoracic ultrasonography or LUS, it was observed that although lung affections were found in all elephants with BCS <3 ($n = 5$), they could also be detected in six out of eight elephants ($n = 6$) that showed similar clinical signs but had BCS ≥3. In addition, four elephants with BCS ≥3 and no clinical signs also showed mild-to-moderate stages of lung pathologies. Of the 28 elephants evaluated, 15 elephants showed lung pathologies upon performing LUS. This indicated that BCS and clinical symptoms are not strictly accurate denominators of pulmonary health, as a few elephants exhibited lung pathologies despite appearing clinically healthy and BCS ≥3 (Table 1).

In elephants with BCS of 4 or above, the image quality was poor due to a thick layer of subcutaneous fat and bulging of skin, increasing the distance of the transducer from the pulmonary parenchyma. In addition, scanning in elephants with dry, very wrinkly or hyperkeratinized skin produced images of reduced quality [26] despite generous application of the acoustic gel. This was a result of increased image attenuation caused by a thick layer of adipose tissue and the dry, hyperkeratinized skin.

The lungs were scanned in the intercostal spaces along the lateral walls of the thoracic cavity [22] only, as they were inaccessible from the ventral thoracic wall. This is because of the unique internal anatomy of elephants caused by an oblique orientation of the diaphragm [4].

3.1 | Normal Lung Appearance

Elephant lungs are highly voluminous organs. While scanning each zone, the cranial regions showed a gradual downward sloping of the pleural line as it progressed towards the apex, indicating the anatomical tapering of the anterior lung. In the middle region, the pleural line appeared horizontally positioned

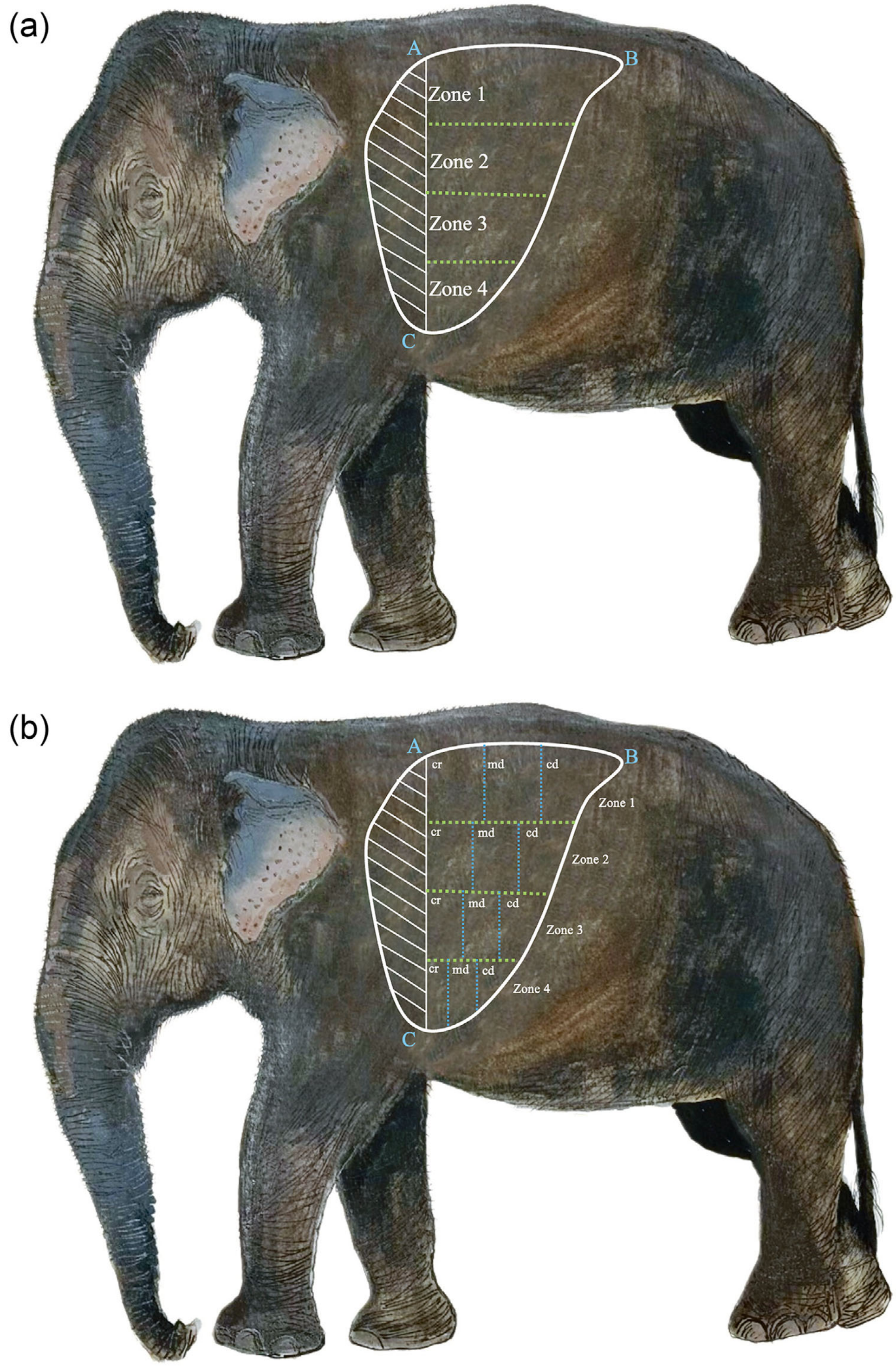

FIGURE 2 | (a) The lateral lung area is outlined (white), with points A, B, and C marking the points of the triangular lung. Three horizontal dotted lines (green) divide the accessible lung into four zones. The inaccessible apical lung region is indicated by the shaded white region. (b) Each zone of the lung is further divided by vertical dotted lines (blue) into cranial (cr), middle (md), and caudal (cd) regions.

under the ribs with no sloping in any zone. In the caudal region, the pleural line would be abruptly discontinued and followed downward with horizontal artifacts (in healthy lung), denoting the caudal border of the lungs.

LUSs are based on artifacts, and every tissue encountered by the sound beam produces characteristic image artifacts. "Wet" and "dry" lungs were denoted by specific artifacts, which enabled their diagnosis [27]. On the lateral side of the pleural line are the ribs, which block the passage of ultrasound and create acoustic shadows or "rib shadow." The rib shadows together with the lung parenchyma in between created the characteristic "bat sign" [28] while viewing the lung with ultrasound in longitudinal section view, parallel to the dorsal plane (Figure 4). The bat sign is a permanent landmark in LUS and could be visualized in all scans, regardless of pulmonary condition [24].

In healthy lung tissue, the ultrasound beam encounters air immediately after crossing the pleural line. This air interface created echogenic horizontal linear artifacts emerging from and parallel to the pleural line (Figure 5). These repetition artifacts are equidistant to each other and are termed "A-lines" [24, 28].

The term "B-lines" refers to comet-tail artifacts generated by an air-fluid mixture that occur when subpleural interlobular septa surrounded by subpleural air-filled alveoli become edematous [29]. The comet tails appeared as long, tapering echogenic cones that decreased in width and amplitude with increasing distance. These bright lines started at the pleural line and traveled in a linear fashion through the field and are termed "lung rockets," and they commonly indicate interstitial syndrome [24, 28, 30] (Figure 6). When the number of B-lines in an intercostal window surpassed 4–5 or showed confluence of multiple rockets with a uniformly bright parenchymal echogenicity, marked pulmonary edema was indicated. Fewer than 4 B-lines were considered non-pathological. Similar findings were described in humans [24] and dogs and cats [31]. Lungs, which were "dry," showed distinct A-lines, whereas the occurrence of several comet-tail artifacts and confluent B-lines indicated a "wet lung." The B-lines could appear localized, homogenous, non-homogeneous, or disseminated, depending on the pathology [32].

FIGURE 3 | Placement of the ultrasound transducer on the lateral thoracic wall during lung ultrasound of an elephant: probe axis directed parallel to the dorsal plane and perpendicular to the median plane.

In clinically healthy lungs, the sliding movement of the visceral pleura against the parietal pleura during inhalation and exhalation is termed "lung slide" and often appreciated as echogenic particulate movement on the pleural line. Lung sliding is a to-and-fro dynamic due to the craniocaudal pulmonary excursion during respiration [33]. In elephants, lung sliding was best appreciated at the caudal border of the lungs at Zones 2 and 3, displaying maximal movement.

Although there exists the popular belief of complete lack of lung sliding in elephants due to the close attachment of their parietal and visceral pleura [1, 2, 5] and respiration being possible only with the movement of the diaphragm and thoracic muscles, notable cranio-caudal sliding movement of the lungs was appreciated during ultrasound, with respect to inhalation and exhalation. This finding, along with studies conducted during necropsies, indicates that although there exist a meshwork of connective tissue attachments between the parietal and visceral pleura in elephants, it does not completely prevent the lungs from sliding.

On average, elephants with healthy lungs showed sliding at a span of 1.5–2 intercostal spaces. The M-mode aided in further understanding this motion in relation to superficial tissues creating a characteristic "seashore sign" (Figure 7). The skin, subcutaneous fat tissue, connective tissue, and muscles were stationary and created horizontal lines, called "waves," whereas the motion of the lung parenchyma during respiration created a granular appearance, called the "sand," hence creating the appearance of a seashore [28, 33]. Lung sliding, physiologically more discrete at the upper parts, could be very discrete in pathological conditions and requires evaluation without any filters. For the application of M-mode, the middle region of Zones 1–3 was preferred, as this region provided an evenly horizontal and uninterrupted pleural line. In the absence of lung sliding, all layers of the tissues on the field of view appeared static, creating horizontal lines across the field under M-mode, creating a "stratosphere sign" [24, 28].

TABLE 1 | Relationship between body condition score (BCS), clinical signs, and lung ultrasound (LUS) findings in 28 elephants.

Sl. no.	Group	No. of elephants	Presence of clinical signs	Lung pathologies detected by LUS
1.	BCS < 3	5	Yes	5
2.	BCS ≥ 3	8	Yes	6
3.	BCS≥	15	No	4
	Total	28	—	15

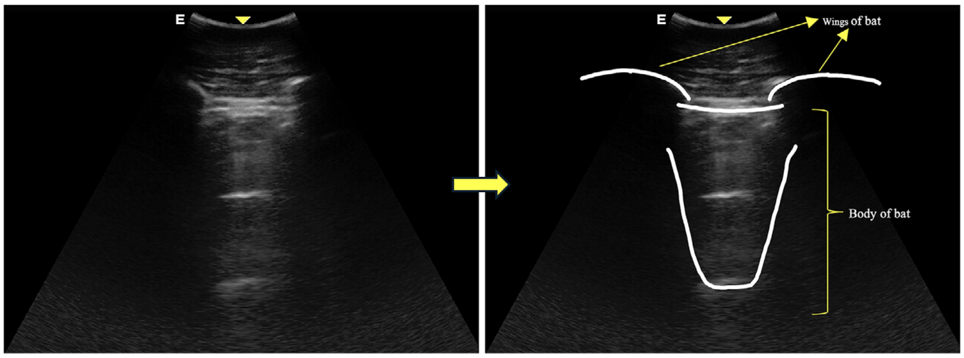

FIGURE 4 | Characteristic appearance of "bat-sign" in lung ultrasound of an elephant. As shown in the image, the characteristic appearance of the lung can be identified as the silhouette of a bat with spread wings, the ribs forming the wings, and the lung parenchyma appearing as the bat's body.

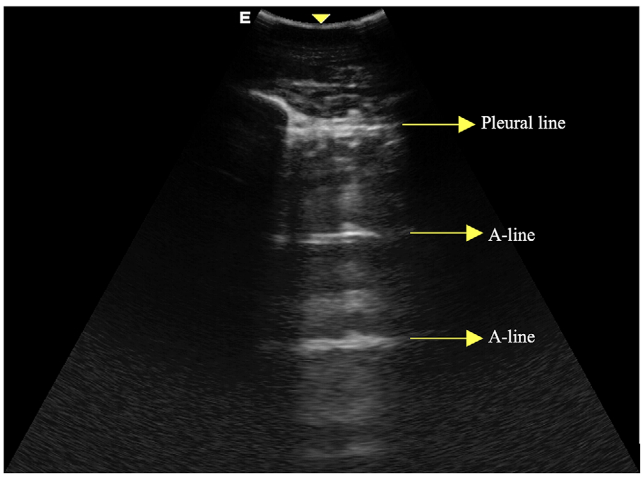

FIGURE 5 | A-lines in lung ultrasound of an elephant: The pleural line consistently represents the parietal pleura. Beneath this line, a horizontal reverberation artifact referred to as the A-lines is typically observed.

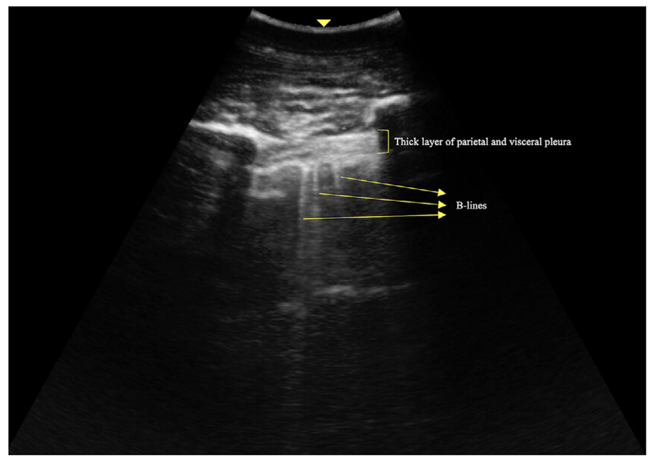

FIGURE 6 | B-lines in lung ultrasound in an elephant: The B-line is consistently characterized as a well-defined, comet-tail artifact that originates from the pleural line and moves synchronously with lung sliding.

3.2 | Interstitial Syndrome

Interstitial syndrome was characterized by multiple lung rockets during examination and was often caused by a singular or combination of conditions such as fibrosis, interstitial pneumonia, and pulmonary edema [34].

In Asian elephants, pulmonary edema was observed to be a common consequence of a chronic left ventricular insufficiency leading to cardiogenic pulmonary edema (CPE) [35, 36] and chronic hypoproteinemia, wherein it was often accompanied by other findings such as ascites and ventral edema.

The B-lines in interstitial syndrome were often the result of juxtaposition of air-filled alveolar spaces with the thickened interstitium (due to fluid accumulation or fibrosis) [34]. In all elephants with interstitial syndrome, the B-lines originated at the pleural line and traversed the field uninterrupted, erasing the A-lines and moving along the lung slide. As edema increased, B-lines became more frequent and adjacent. Very severe pulmonary edema caused confluence of multiple B-lines creating a hyperechoic appearance (Figure 8) of the lung within the intercostal space in view, called the "white lung" [24, 28, 37]. Chronic pulmonary edema increases alveolar surface tension due to elevated surfactant activity, eventually leading to atelectasis. This could be detected as a "lung pulse" with LUS [24]. In dynamic imaging, a lung pulse appeared as a rhythmic movement of the pleural line contiguous with cardiac pulsations. In elephants, lung-pulse was observed after chronic pulmonary edema, with a poor response to diuretics, and was detected in Zones 3 and 4, with more evident pulsatile activity in the cranial thoracic region, often bilaterally.

3.3 | Pulmonary Consolidation

Consolidations in the lung were consistently found to reach the pleura in elephants and could be readily detected using LUS. Pulmonary consolidation might manifest as wedge-shaped opacities extending from the pleural surface, as discrete nodules, or as involvement of an entire lung lobe [38]. These usually manifested in three forms:

Mild pulmonary consolidation: These appeared as small, hypoechoic regions with indistinct margins, throwing comet-tails to the far field (Figure 9), often with subpleural consolidations (SubPL-cons) of below 1 cm diameter.

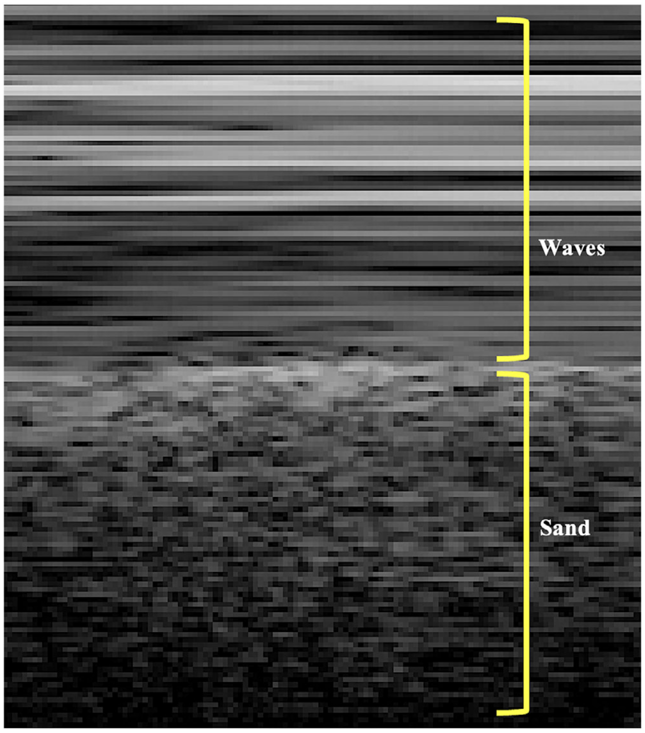

FIGURE 7 | Seashore sign in M-mode lung ultrasound of an elephant: Superior to the pleural line, the static chest wall exhibits a stratified or layered echotexture. In contrast, the region inferior to the pleural line demonstrates a granular or "sandy" appearance.

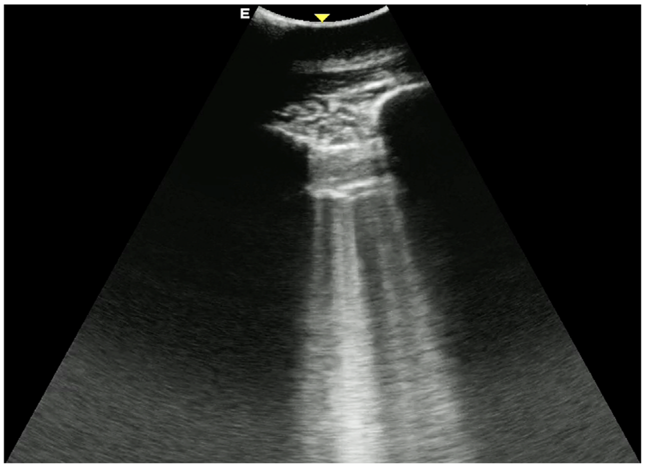

FIGURE 8 | Multiple B-lines covering the majority of the intercostal space in an elephant, creating the image of a "white lung" detected using lung ultrasound.

Tissue sign: It was also termed "hepatization" and was observed when the pulmonary parenchyma was filled with fluid and manifested the echogenicity of the liver (Figure 10). In severe cases, pleural effusion might accompany [28].

Shred sign: In partial or incomplete infiltration of fluid across the lung, there were air spaces occurring in frequent intervals. This exhibited poorly defined regions of lowered echogenicity, neighboring aerated pulmonary tissue displaying sliding and B-

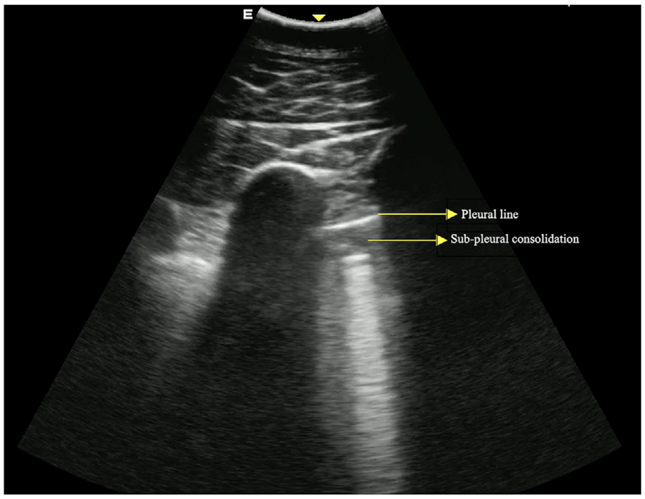

FIGURE 9 | Mild (subpleural) pulmonary consolidation in lung ultrasound of an elephant.

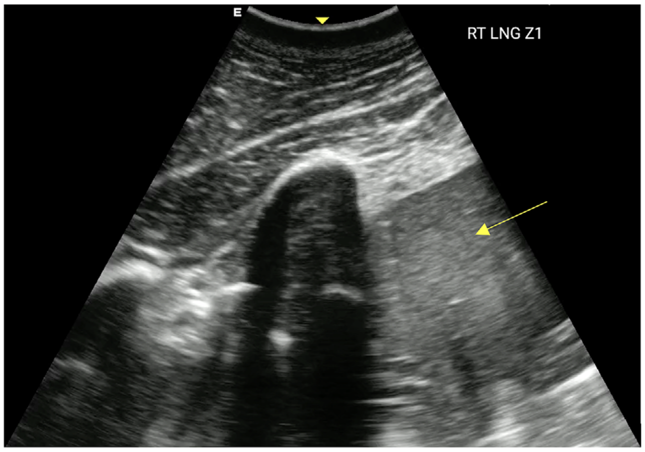

FIGURE 10 | Tissue sign: lung "hepatization" detected in the cranial region (arrow) of Zone 1 on the right lung of an elephant.

lines (Figure 11). The junction between fluid-filled and aerated lungs did not appear well demarcated. Shred sign in lungs was indicative of pneumonia [24].

3.4 | Bronchograms

LUS was used to assess the integrity of the visible passageways in a diseased lung, as evidenced by air or fluid bronchograms. These signs helped in the diagnosis of various lung pathologies.

Air bronchogram: Bright echogenic appearances, which might be punctiform or linear based on their alignment to the transducer, were surrounded by consolidated lung tissue (Figure 12).

Fluid bronchogram: Anechoic tubular structures surrounded by consolidated lung tissue, representing fluid-filled bronchi or bronchioles [28, 39]. However, it was often challenging to distinguish them from pulmonary blood vessels in elephants due to their great distance from the transducer, creating

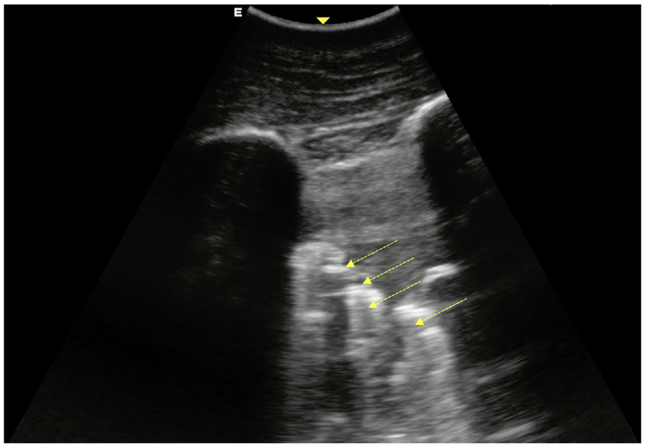

FIGURE 11 | "Shred sign," indicating marked, interrupted consolidations (arrows) in lung ultrasound of an elephant.

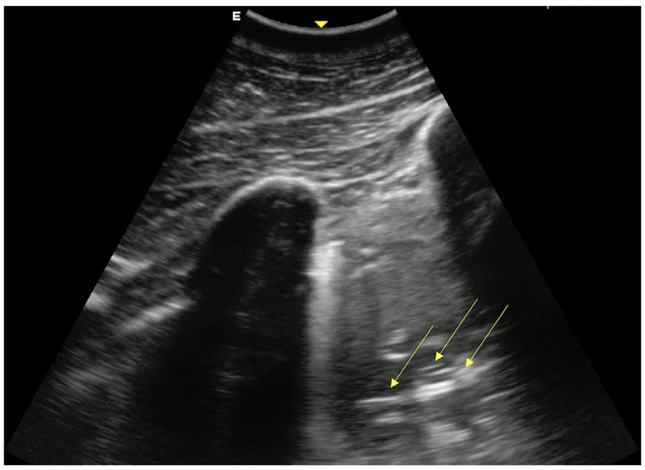

FIGURE 12 | Air bronchogram (arrows) in lung ultrasound of an elephant at the cranial region of Zone 1 in the right lung.

very weak signals when viewed with color Doppler image mode.

3.5 | Pneumothorax

LUS demonstrated high sensitivity for detecting pneumothorax and could be performed within minutes. The region of the lung affected by pneumothorax showed alterations, such as abolished lung sliding with a motionless pleural line [22] in B-mode and a stratosphere sign in M-mode [30]. There were no B-lines, and "lung point" could be detected, as the point of intersection between the sliding lung and static, non-sliding lung [24, 28, 31]. Air, being non-dependent, accumulated in the dorsal region of the thoracic cavity in elephants. Placement of the probe preferably in Zone 1, or in Zone 2 if thick, hyperkeratinized skin is present in Zone 1, and studying lung sliding could help confirm a pneumothorax. Identification of the lung point was pathognomonic for pneumothorax; however, its detection was challenging in chronic cases and was further complicated by the substantial size of the elephant lung. Complex pneumothoraces with extensive adherences did not exhibit lung point, as a fully collapsed lobe could not always reach the thoracic wall [40].

3.6 | Pleural Effusion

In elephants, LUS provided a 90% sensitivity and 95% specificity to pleural effusion and helped determine the nature of fluid in the distal pleural cavity. Simple pleural effusions appeared anechoic and were usually transudates, whereas complex effusions appeared mildly to moderately echogenic and were usually exudative. Pleural line abnormalities and pleural effusions were always associated with areas of confluent B-line artifacts, often accompanied by lung consolidation [27]. In elephants with marked hypoproteinemia, pleural effusions were detected and accompanied by ascites.

Pleural effusion resulted in the accumulation of fluid within the potential space between the parietal and visceral pleura. This was observed in B-mode imaging as a "quad sign" (Figure 13), a rectangular or quadrilateral shape outlined by the parietal and visceral pleura at the top and bottom, and the rib shadows on the sides [28, 30]. In M-mode ultrasonography, pleural effusion produced a characteristic wavy pattern at the level of the visceral pleura, known as the "sinusoid sign" [30, 24]. In the current study, elephants with chronic clinical symptoms and three with electrocardiography-detected cardiac functional insufficiency showed pleural effusion of varying degrees.

Pleural effusion was detected only in a narrow window at the dependent region (Zone 4) of the thoracic cavity in standing elephants, as fluid traveled downward due to gravitational pull. In addition, the parietal and visceral pleura appeared thickest at the dorsal and lateral regions (Zones 1, 2, and 3) of the lung, with little to no space in between for accommodation of free fluid.

3.7 | LUS Score

In elephants, the expansive lungs were divided into 12 regions of interest (ROIs) on each side, and each ROI was imaged in real time using LUS to assess pulmonary health [15]. On the basis of the assessment of aeration, each ROI was then assigned a number between 0 and 3 (Figure 14). This semi-quantitative scoring system was called an LUS, and the total score could range from 0 to 72, after combining the results from all 24 ROIs.

The LUSs for each ROI were determined by the type of lesion as well as the qualitative aeration (Table 2).

With the classification of the LUSs, a scorecard was then prepared for each elephant that was evaluated. Scores were assigned to each ROI of the left and right lung, then the scores from both lungs were added to obtain the total LUSs (T-LUSs) (Table 3).

In this study, a cut-off was designated for the T-LUSs:

- T-LUSs 0 = normal aeration in all parts of the lungs
- T-LUSs 1–12 = moderate aeration loss with mild pulmonary involvement
- T-LUSs 13–24 = severe aeration loss with moderate to severe pathology
- T-LUSs >24 = complete aeration loss with severe pathology

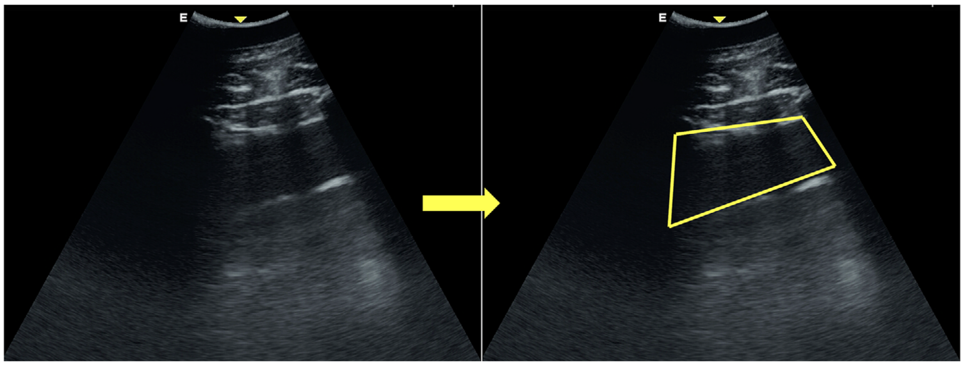

FIGURE 13 | Pleural effusion detected using lung ultrasound in an elephant, characterized by the "quad sign" formed by the parietal and visceral pleura on the top and bottom and laterally by the rib shadows.

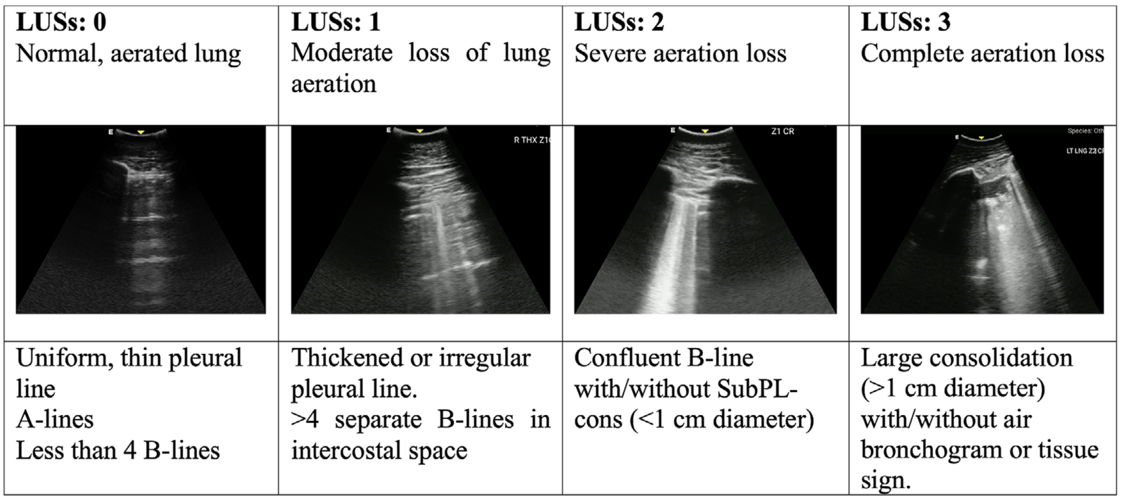

FIGURE 14 | Categorization of lung ultrasound images as per their respective lung ultrasound scores (LUSs) in elephants.

TABLE 2 | Lung ultrasound scores (LUSs) in elephants according to the sonographic pattern.

LUSs	Status of lung aeration	LUS appearance	Pathological conditions
0	Normal aeration	• Well-defined, uniform pleural line • A-lines • B-lines <4 in number • Lung sliding	None
1	Moderate loss	• Thickened, irregular pleural line • A minimum of four discrete B-lines covering <50% of one intercostal space	Interstitial syndrome, localized pulmonary edema, or SubPL-cons
2	Severe loss	• Confluent B-lines covering >50% of the intercostal space • Small consolidations	Alveolar edema, CPE, and pneumonia
3	Complete loss	• Thick, irregular pleural line may appear discontinued • Tissue sign with or without air bronchogram • Reduced or no lung sliding	Pneumonia, pulmonary consolidation, and pneumothorax

Abbreviations: CPE, cardiogenic pulmonary edema; SubPL-cons, subpleural consolidations.

TABLE 3 | Score card of lung ultrasound in elephants for a detailed semi-quantitative respiratory health assessment.

Left lung	Left lung	Left lung	Right lung	Right lung	Right lung
Zone (Z)	Region (cr = cranial, md = middle, cd = caudal)	Score (0–3)	Zone (Z)	Region (cr = cranial, md = middle, cd = caudal)	Score (0–3)
Z1	Z1-cr		Z1	Z1-cr	
Z1	Z1-md		Z1	Z1-md	
Z1	Z1-cd		Z1	Z1-cd	
Z2	Z2-cr		Z2	Z2-cr	
Z2	Z2-md		Z2	Z2-md	
Z2	Z2-cd		Z2	Z2-cd	
Z3	Z3-cr		Z3	Z3-cr	
Z3	Z3-md		Z3	Z3-md	
Z3	Z3-cd		Z3	Z3-cd	
Z4	Z4-cr		Z4	Z4-cr	
Z4	Z4-md		Z4	Z4-md	
Z4	Z4-cd		Z4	Z4-cd	
Left LUSs	Left LUSs		Right LUSs	Right LUSs	
T-LUSs (Left LUSs + Right LUSs)=	**T-LUSs** (Left LUSs + Right LUSs)=	**T-LUSs** (Left LUSs + Right LUSs)=	**T-LUSs** (Left LUSs + Right LUSs)=	**T-LUSs** (Left LUSs + Right LUSs)=	**T-LUSs** (Left LUSs + Right LUSs)=

Abbreviation: T-LUSs, total lung ultrasound scores.

TABLE 4 | Clinical signs, LUS-detected lung pathology, and total lung ultrasound scores (T-LUSs) in 28 elephants.

Elephant no.	Sex	BCS	Clinical signs (Yes: +, No: −)	Pathology in LUS (Yes: +, No: −)	T-LUSs
	F	3	+	+	38
	M	2	+	+	8
	M	4	−	−	0
	F	2	+	+	54
	F	4	+	+	13
	F	4	−	−	0
	F	4	−	−	0
	F	3	−	−	0
	F	2	+	+	63
	F	3	+	+	15
	F	2	+	+	40
	F	4	+	+	26
	F	4	−	+	3
	F	4	−	−	0
	F	2	+	+	39
	F	4	−	−	0
	F	4	+	+	19
	F	4	−	−	0
	F	3	−	−	0
	F	3	+	+	15
	F	3	−	−	0
	F	4	−	−	0
	F	4	−	+	4
	F	3	−	−	0
	F	3	−	−	0
	F	4	−	−	0
	F	4	−	+	14
	F	3	−	+	7

Abbreviation: BCS, body condition score.

A summary of the elephants in this study was tabulated (Table 4) with respect to their sex, age, clinical signs indicative of respiratory illness, BCS, presence of lung pathology on ultrasound, and their respective T-LUSs.

It is evident from Table 4 that LUS aided in the detection of pulmonary conditions in four elephants that did not exhibit any clinical signs indicative of respiratory insufficiency. This demonstrated the capacity of LUS as a rapid and noninvasive technique for the detection of subclinical lung pathology in elephants.

The T-LUSs category for the elephants studied was tabulated in relation to their BCS scores (Table 5).

3.8 | Challenges of LUS in Elephants

In this study, conducted over the span of 22 months, two prominent challenges were observed in elephants with respect to LUS, which are species-specific according to the authors:

1. Large lung volume: The elephant lungs are highly voluminous organs with a large span tracing along the medial surfaces of the lateral walls of the thoracic cavity. The thoracic ribs framing the chest walls are closely spaced with narrow intercostal spaces, thus providing relatively small acoustic windows. This made a detailed study encompassing each of the 24 ROIs tedious and time-consuming. Additionally, despite LUS acquiring images up to a depth of 45 cm, the

TABLE 5 | Distribution of total lung ultrasound scores (T-LUSs) in elephants with LUS-detected lung pathology.

Group	No. of elephants	T-LUSs category (score range)	No. of elephants
BCS <3	5	Mild (TLUSs 1–12)	1
BCS <3	5	Severe (T-LUSs > 24)	4
BCS ≥3 with clinical signs	6	Moderate (T-LUSs 13–24)	4
BCS ≥3 with clinical signs	6	Severe (T-LUSs > 24)	2
BCS ≥3 without clinical signs	4	Mild (TLUSs 1–12)	3
BCS ≥3 without clinical signs	4	Moderate (T-LUSs 13–24)	1

Abbreviation: BCS, body condition score.

large girth of the elephant's chest still posed the possibility of deeper lesions, such as masses or other anomalies, going undetected. However, the location of the majority of pulmonary pathologies at the periphery and pathognomonic artifacts arising from the pleural line (>95%) ensured high chances of their detection.

2. Pectoral limb superimposition: The apical ends of both lungs in elephants were not accessible with ultrasound due to the superimposition of the craniolateral thorax with the pectoral limbs.

4 | Conclusion

This study established LUS as a valuable real-time imaging modality for evaluating pulmonary health in Asian elephants. LUS demonstrated high sensitivity in detecting pathologies, even in apparently healthy elephants without clinical signs indicating respiratory illness, highlighting its diagnostic advantage over conventional assessments based solely on body condition scoring and clinical presentation. In addition, LUS proved reliable in the detection of pulmonary pathologies in elephants, as these conditions tend not to manifest in routine blood work, and conventional radiological procedures such as chest x-ray in individuals above calf-size, CT scan, or MRI used widely in other species are not applicable in elephants.

Consistent thoracic zones were mapped to enhance lesion localization, and a semi-quantitative LUS was developed. This scoring system enabled rapid, objective evaluation of lung aeration across 24 ROIs, facilitating classification of disease severity.

Despite species-specific challenges such as large lung volume and narrow intercostal spaces, LUS consistently revealed key sonographic signs, including A-lines, B-lines, and lung sliding. These findings were instrumental in the assessment of lung health and detecting conditions like pulmonary edema, consolidation, pneumothorax, and pleural effusion.

Therefore, LUS emerges as a noninvasive, field-adaptable imaging technique that can significantly improve respiratory monitoring and disease management in elephants. LUS provides the opportunity for antemortem detection of lung pathologies and allows veterinarians the window of opportunity for prompt intervention. Its application holds promise for advancing both clinical care and conservation efforts for this endangered species. The authors recommend that LUS may be included in the routine health assessment of Asian elephants under human care.

Author Contributions

Vaisakh Viswam: writing – review and editing. **Akshay Ghatare**: writing – review and editing. **Yaduraj Khadpekar**: writing – review and editing. **Nirmali Sarma**: conceptualization, methodology, investigation, supervision, writing – review and editing, writing – original draft. **Niraj Dahe**: writing – review and editing. **Nikorn Thongtip**: writing – review and editing. **Tenzing L. Lachenpa**: investigation, writing – review and editing, methodology. **Jahan Ahmed**: writing – review and editing. **Shubham Patil**: writing – review and editing. **Govind Shankar**: writing – review and editing.

Acknowledgments

The authors would like to express their immense gratitude to Mr. Vivaan Karani, Mr. Aakash Pratap Singh, Dr. Brij Kishore Gupta, Mr. Neeraj Sangwan, and the entire management team of Radhe Krishna Temple Elephant Welfare Trust, Vantara, for their consistent support and facilitation throughout the course of this work. Special thanks to Kushal Konwar Sarma for his guidance and encouragement throughout the period of this study. The authors are also grateful to the veterinary assistants Mr. Suryakant Patil, Mr. Ajinath Munde, Mr. Amar Gharat, Mr. Jigar Prajapati, Mr. Sachin Donde, Mr. Vikee Surwase, Mr. Pritesh Tayade, Mr. Chetan Thomare, Mr. Jitendra Deshpande, Mr. Atish Shinde, and Mr. Jagdish Choudhary for the technical support in the procedures. The authors express their gratitude to Mr. Michael Cruz, Mr. Edsel Cortez, their team of dedicated trainers, and the elephant keepers who have been of immense assistance in desensitizing the elephants to the procedure, thus enabling their cooperation. The authors also thank the biologists Ms. Kunj Joshi, Ms. Krupa Jamdar, Mr. Ashik Shybu, and Ms. Aradhya Siddheish for their association with this work. This study was made possible through the generous financial support of the Reliance Foundation.

Conflicts of Interest

The authors declare no conflicts of interest.

Data Availability Statement

Readers seeking further information may contact the corresponding author, Nirmali Sarma, via email—dr.ninasarma@outlook.com.

References

1. J. B. West, "Snorkel Breathing in the Elephant Explains the Unique Anatomy of Its Pleura," *Respiration Physiology* 126, no. 1 (2001): 1–8.

2. E. C. Amoroso, K. J. Franklin, and M. M. L. Prichard, "Observations on the Cardio-Vascular System and Lungs of an African Elephant Foetus," *Journal of Anatomy* 76, no. Pt 1 (1941): 100–111.

3. K. Sajjarengpong, A. Adirekthaworn, and P. Uthaichotiwan, "The Anatomy and Radiography of THE Lungs of a Stillborn Asian Elephant (*Elephas maximus* indicus)," *Thai Journal of Veterinary Medicine* 35, no. 1 (2005): 67–72.

4. R. E. Brown, J. P. Butler, J. J. Godleski, and S. H. Loring, "The Elephant's Respiratory System: Adaptations to Gravitational Stress," *Respiration Physiology* 109, no. 2 (1997): 177–194.

5. C. V. Rajani, K. P. Surjith, H. S. Patki, et al., "Comparative Morphology of the Larynx, Trachea and Lungs of Asian Elephant (*Elephas maximus* Indicus) and Domestic Animals," *Indian Journal of Veterinary Anatomy* 31, no. 1 (2019): 21–23.

6. A. Ramanathan and A. Mallapur, "A Visual Health Assessment of Captive Asian Elephants (*Elephas maximus*) Housed in India," *Journal of Zoo and Wildlife Medicine* 39, no. 2 (2008): 148–154.

7. C. Doyle, H. Rally, L. O'Brien, M. Tennison, L. Marino, and B. Jacobs, "Continuing Challenges of Elephant Captivity: The Captive Environment, Health Issues, and Welfare Implications," *PeerJ* 12 (2024): e18161.

8. S. K. Mikota and J. N. Maslow, "Tuberculosis at the Human–Animal Interface: An Emerging Disease of Elephants," *Tuberculosis* 91, no. 3 (2011): 208–211.

9. J. Payeur, D. Whipple, C. Thoen, D. S. Davis, and C. Sedgwick, "Section II: Radiology," *Biology, Medicine, and Surgery of Elephants* 26 (2006): 192.

10. J. R. Zuba and K. R. Mama, "Elephants," in *Zoo Animal and Wildlife Immobilization and Anesthesia* (John Wiley & Sons, 2025).

11. A. Armenise, "Point-of-Care Lung Ultrasound in Small Animal Emergency and Critical Care Medicine: A Clinical Review," *Animals* 15, no. 1 (2025): 106.

12. R. Hermes, J. Saragusty, I. Moser, et al., "Bronchoalveolar Lavage for Diagnosis of Tuberculosis Infection in Elephants," *Epidemiology & Infection* 146, no. 4 (2018): 481–488.

13. I. Lueders and C. Stremme, "Construction of a Full Mouth Speculum Facilitating Oral Examinations, Bronchoscopy and Gastric Tubing in Elephants," *Tierärztliche Praxis Ausgabe G: Großtiere/Nutztiere* 50, no. 2 (2022): 86–90.

14. G. R. Lisciandro, "The Role of Lung Ultrasound for the Small Animal Practitioner," *Veterinary Clinics: Small Animal Practice* 51, no. 5 (2021): 1023–1045.

15. S. Oricco, D. Medico, I. Tommasi, R. M. Bini, and R. Rabozzi, "Lung Ultrasound Score in Dogs and Cats: A Reliability Study," *Journal of Veterinary Internal Medicine* 38, no. 1 (2024): 336–345.

16. S. R. Boysen and G. R. Lisciandro, "The Use of Point-of-Care Ultrasound (POCUS) in Small Animal Emergency Medicine," *Journal of Veterinary Emergency and Critical Care* 30, no. 1 (2020): 16–31.

17. S. Reyes-Long, M. Gutierrez, D. Clavijo-Cornejo, et al., "Subclinical Interstitial Lung Disease in Patients With Systemic Sclerosis. A Pilot Study on the Role of Ultrasound. Intersticiopatía Pulmonar Subclínica en Pacientes Con Esclerosis Sistémica. Estudio Piloto sobre el Papel Del Ultrasonido," *Reumatologia Clinica* 17, no. 3 (2021): 144–149.

18. R. Sargo, I. Tomé, F. Silva, and M. Ginja, "Diagnostic Accuracy of Lung Ultrasound in Rabbit Subclinical Lung Lesions," *Veterinary Sciences* 12, no. 4 (2025): 340.

19. J. N. Maslow and S. K. Mikota, "Tuberculosis in Elephants—A Reemergent Disease: Diagnostic Dilemmas, the Natural History of Infection, and New Immunological Tools," *Veterinary Pathology* 52, no. 3 (2015): 437–440.

20. K. A. Morfeld, C. L. Meehan, J. N. Hogan, and J. L. Brown, "Assessment of Body Condition in African (*Loxodonta africana*) and Asian (*Elephas maximus*) Elephants in North American Zoos and Management Practices Associated With High Body Condition Scores," *PLoS ONE* 11, no. 7 (2016): e0155146.

21. T. B. Hildebrandt, "Reproductive and Diagnostic Ultrasonography," in *Biology, Medicine, and Surgery of Elephants* (John Wiley & Sons, 2006): 357–376.

22. L. F. Feitoza, B. J. White, and R. L. Larson, "Thoracic Ultrasound in Cattle: Methods, Diagnostics, and Prognostics," *Veterinary Sciences* 12, no. 1 (2025): 16.

23. E. Timsit, N. Tison, C. W. Booker, and S. Buczinski, "Association of Lung Lesions Measured by Thoracic Ultrasonography at First Diagnosis of Bronchopneumonia With Relapse Rate and Growth Performance in Feedlot Cattle," *Journal of Veterinary Internal Medicine* 33, no. 3 (2019): 1540–1546.

24. D. A. Lichtenstein, "Lung Ultrasound in the Critically Ill," *Annals of Intensive Care* 4, no. 1 (2014): 1.

25. P. Reinhold, B. Rabeling, H. Günther, and D. Schimmel, "Comparative Evaluation of Ultrasonography and Lung Function Testing With the Clinical Signs and Pathology of Calves Inoculated Experimentally With *Pasteurella multocida*," *Veterinary Record* 150 (2002): 109–114.

26. T. B. Hildebrandt and J. Saragusty, "Use of Ultrasonography in Wildlife Species," *Fowler's Zoo and Wild Animal Medicine* 8 (2015): 714–723.

27. C. F. Dietrich, G. Mathis, M. Blaivas, et al., "Lung Artefacts and Their Use," *Medical Ultrasonography* 18, no. 4 (2016): 488–499.

28. A. Miller, "Practical Approach to Lung Ultrasound," *BJA Education* 16, no. 2 (2016): 39–45.

29. D. A. Lichtenstein, G. A. Meziere, J. F. Lagoueyte, P. Biderman, I. Goldstein, and A. Gepner, "A-Lines and B-Lines: Lung Ultrasound as a Bedside Tool for Predicting Pulmonary Artery Occlusion Pressure in the Critically Ill," *Chest* 136, no. 4 (2009): 1014–1020.

30. A. Murali, A. Prakash, R. Dixit, M. Juneja, and N. Kumar, "Lung Ultrasound for Evaluation of Dyspnea: A Pictorial Review," *Acute and Critical Care* 37, no. 4 (2022): 502–515.

31. L. Cole, M. Pivetta, and K. Humm, "Diagnostic Accuracy of a Lung Ultrasound Protocol (Vet BLUE) for Detection of Pleural Fluid, Pneumothorax and Lung Pathology in Dogs and Cats," *Journal of Small Animal Practice* 62, no. 3 (2021): 178–186.

32. G. R. Lisciandro and J. M. Gambino, *Diagnostic Imaging: Point-of-Care Ultrasound, an Issue of Veterinary Clinics of North America: Small Animal Practice, E-Book* (Elsevier Health Sciences, 2021).

33. J. K. Kealy, H. McAllister, and J. P. Graham, *Diagnostic Radiology and Ultrasonography of the Dog and Cat* (Elsevier Health Sciences, 2010).

34. D. A. Lichtenstein, "Lung and Interstitial Syndrome," in *Whole Body Ultrasonography in the Critically Ill* (Springer Berlin Heidelberg, 2010).

35. L. Dobbe, R. Rahman, M. Elmassry, P. Paz, and K. Nugent, "Cardiogenic Pulmonary Edema," *American Journal of the Medical Sciences* 358, no. 6 (2019): 389–397.

36. C. Zanza, F. Saglietti, M. Tesauro, et al., "Cardiogenic Pulmonary Edema in Emergency Medicine," *Advances in Respiratory Medicine* 91, no. 5 (2023): 445–463.

37. G. Soldati, A. Smargiassi, R. Inchingolo, et al., "Is There a Role for Lung Ultrasound During the COVID-19 Pandemic?" *Journal of Ultrasound in Medicine: Official Journal of the American Institute of Ultrasound in Medicine* 39, no. 7 (2020): 1459–1462.

38. T. L. Ollivett and S. Buczinski, "On-Farm Use of Ultrasonography for Bovine Respiratory Disease," *Veterinary Clinics of North America: Food Animal Practice* 32 (2016): 19–35.

39. G. Volpicelli, "Lung Sonography," *Journal of Ultrasound in Medicine* 32, no. 1 (2013): 165–171.

40. S. Mongodi, G. Salve, and F. Mojoli, "Pneumothorax," in *Basic Ultrasound Skills "Head to Toe" for General Intensivists* (Springer International Publishing, 2023).